Pure α-Fe Coated by an $Fe_{1-x}B_x$ Alloy

N. Duxin,[†,‡] O. Stephan,[§] C. Petit,[†,‡] P. Bonville,[⊥] C. Colliex,*[,§] and M. P. Pileni*[,†,‡]

Université Pierre et Marie Curie, Laboratoire "Structure et Réactivité des Systèmes Interfaciaux", URA CNRS 1662, BP 52, 4 place Jussieu, 75005 Paris, France; CEA-DSM-DRECAM Service de Chimie Moléculaire, CEA Saclay, 91191 Gif sur Yvette, Cedex, France; Université Paris-Sud, Laboratoire de Physique des Solides, URA 002, Bât 510, 91450 Orsay Cedex, France; and CEA-DSM-DRECAM Service de Physique de l'Etat Condensé, CEA Saclay, 91191 Gif sur Yvette, Cedex, France

Received March 18, 1997. Revised Manuscript Received June 16, 1997[⊗]

Functionalized surfactant as iron(II) bis(ethyl-2-hexyl)sulfosuccinate, $Fe(AOT)_2$, is used to synthesize metallic nanoparticles of α-Fe and of a Fe−B alloy through chemical reduction with $NaBH_4$. The particles are observed by transmission electron microscopy and characterized by X-ray diffraction, electron diffraction, Mössbauer spectroscopy, and electron energy loss spectrometry. The room-temperature magnetization curve is also presented.

Introduction

Nanostructured materials, because of their large specific surface often have unique wide range of applications.[1−4] They can be electrical, structural, and magnetic properties, including information storage, color imaging, bioprocessing, magnetic refrigeration, and ferrofluids.

We usually assume that nanostructured materials exhibit a unique type of disorder, with very low-energy regions (crystallites) existing at the extense of higher energy boundary, interface or surface regions.[5] Magnetic nanostructure studies combine a broad range of synthetic and investigative techniques from physics, chemistry, and materials science. In the best case, these studies not only provide information about the structural and magnetic properties but also improve understanding of the synthesis technique. The correlation between nanostructure and magnetic properties suggests a classification of nanostructure morphologies. At one extreme are systems of isolated particles with nanoscale diameters which are noninteracting systems and derive their unique magnetic properties strictly from the reduced size of the components with no contribution from interparticles interactions. At the other extreme are bulk materials with nanoscale structure in which a significant fraction of the sample is composed of grain boundaries and interfaces.

Amorphous transition metal−boron alloys have been studied extensively in the bulk phase.[6−8] Various well-known techniques of preparation of these alloys have been used such as cosputtering of the elements on a substrate, quenching a liquid to a temperature below the glass transition, solvated metallic atom deposition, and gas evaporation. Finally, the chemical route was used consisting of the reduction of aqueous metallic salts, M^{2+} by sodium borohydride, $NaBH_4$. By using the latter procedure, the amount of boron in the materials strongly depends on the preparation parameters such as temperature, concentration, pH, solvent, and mixing procedure. Large studies on syntheses, structural, and magnetic properties were done on such materials.[9−20] The alloy formation was demonstrated by a macroscopic technique, and no local studies were performed.

In the present paper, we develop a new synthesis with diphasic systems. This method is the reduction of the iron(II) bis-(ethyl-2-hexyl)sulfosuccinate surfactant, $Fe(AOT)_2$, by $NaBH_4$. We use macroscopic (transmission electron microscopy, X-ray diffraction, and Mössbauer spectroscopy) and nanoscopic (electron energy loss spectrometry) techniques to describe the material formed by using such a synthetic mode. We demonstrate the formation of α-Fe particles coated by iron alloys.

* To whom correspondence should be addressed.
† Université Pierre et Marie Curie.
‡ Service de Chimie Moléculaire.
§ Université Paris-Snd.
⊥ Service de Physique de l'Etat Condensé.
⊗ Abstract published in *Advance ACS Abstracts,* September 15, 1997.

(1) Molnar, A.; Smith, G. V.; Bartok, M.; *Adv. Catal.* **1989**, *36*, 329.
(2) Wade, R. C.; Holah, D. G.; Hughes, A. N.; Hui, B. C. *Catal. Rev. Sci. Eng.* **1976**, *14*, 211.
(3) Shen, J.; Li, Z.; Zhang, Q.; Chen, Y.; Bao, Q. *Proceeding of the 10th International Congress on catalysis, Budapest, Hungary* **1992**.
(4) Linderoth, S.; Morup, S. *J. Appl. Phys.* **1991**, *69−8*, 5256.
(5) Gleiter, H. *Prog. Mater. Sci.* **1989**, *33*, 223.
(6) Hasegawa, R.; Ray, R. *J. Appl. Phys.* **1978**, *49*, 4174.
(7) Kernizan, C. F.; Klabunde, K. H.; Sorensen, C. M.; Hadjipanayis, G. C. *J. Appl. Phys.* **1990**, *67*, 5897.
(8) Hayashi, C. *J. Vac. Sci., A5* **1987**, 1375.
(9) Mountjoy, G.; Corrias, A.; Gaskell, P. H. *J. Non-Cryst. Solids* **1995**, *192*, 616.
(10) Corrias, A.; Ennas, G.; Licheri, G.; Maronjiu, G.; Pashina, G. *Chem. Mater.* **1990**, *2*, 363.
(11) Linderoth, S.; Morup, S.; Koch, C. J. W.; Wells, S.; Charles, S. W.; van Wonterghem, J.; Meaghe, A. *J. Phys. Colloq.* **1988**, *49*, C8−1369.
(12) Nafis, S.; Hadjipanayis, G. C.; Sorensen, C. M.; Klabunde, K. J. *IEEE Trans. Magn. Magn.* **1989**, *25*, 3641.
(13) Yiping, L.; Hadjipanayis, G. C.; Sorensen, C. M.; Klabunde, K. J. *J. Magn. Magn. Mater.* **1989**, *79*, 321.
(14) Linderoth, S.; Morup, S.; Meagher, A.; Larsen, J.; Bentzon, M. D. *J. Magn. Magn. Mater.* **1989**, *81*, 138.
(15) Saida, J.; Inoue, A.; Masumoto, T. *Metallurgical Trans. A* **1993**, *22*, 2125.
(16) Saida, J.; Inoue, A.; Masumoto, T. *Mater. Sci. Eng.* **1994**, *A179/A180*, 577.
(17) Jiang, J.; Dezsi, I.; Gonser, U.; Weissmuller, J. *J. Non-Cryst. Solids* **1990**, *116*, 247.
(18) Glavee, G. N.; Klabunde, K. J.; Sorensen, C. M.; Hadjipanayis, G. C. *Langmuir* **1993**, *9*, 163.
(19) Glavee, G. N.; Klabunde, K. J.; Sorensen, C. M.; Hadjipanayis, G. C. *Langmuir* **1994**, *10*, 4726.
(20) Glavee, G. N.; Klabunde, K. J.; Sorensen, C. M.; Hadjipanayis, G. C. *Inorg. Chem.* **1995**, *34*, 28.

S0897-4756(97)00156-7 CCC: $14.00

Experimental Procedure

Products. Sodium bis-(ethyl-2-hexyl)sulfosuccinate, AOT, was purchased from Sigma, isooctane was obtained from Fluka (99.5% puriss), and $NaBH_4$ was from Alpha Products. All chemicals were used without further purification.

Singly distilled water was passed through a Millipore MilliQ system cartridge until its resistivity reached 18 MΩ cm.

Functionalized Surfactants. Syntheses of iron(II) bis-(ethyl-2-hexyl)sulfosuccinate, $Fe(AOT)_2$, have been described previously.[21]

Magnetization curves were obtained with a commercial alternative gradient field magnetometer (AGFM) operating at room temperature in a field up to 1.8 T.

X-ray diffraction (XRD) measurements were carried out by using a Stoe Stadi P goniometer with a Siemens Kristalloflex-X-ray generator using cobalt anticathode driven by a personal computer through the Daco-PM interface.

Transmission Electron Microscopy (TEM) and Electron Diffraction (ED). A drop of the solution is evaporated on a microscope grid in an inert atmosphere (N_2) and the TEM pattern were obtained by using a JEOL electron microscope (Model JEOL 100 CX. 2).

Electron Energy Loss Spectrometry (EELS). The EELS data were recorded using a scanning transmission electron microscope (STEM; VG HB 501 equipped with a Gatan 666 parallel EELS spectrometer) on the same specimen as observed previously in normal TEM work.

The electron energy loss spectroscopy, EELS, measures the energy loss suffered by high-energy incident electrons transmitted across the specimen.[22]

Mössbauer Experiments. The Mössbauer spectra were recorded using a ^{57}Co*:Rh γ-ray source (E_0 = 14.4 keV) mounted on an electromagnetic drive with a triangular velocity signal. The spectra were least-squares fitted to get the hyperfine parameters (isomer shift δ, quadrupolar splitting Δ, and hyperfine field H_{hf}). In some cases, we observed a broad hyperfine field distribution that was fitted using either a histogram of hyperfine fields with free weights or a Gaussian distribution.

We shall recall briefly the main characteristics of the ^{57}Fe Mössbauer spectra of iron oxides and iron metallic alloys. The isomer shift values (δ) are given with respect to α-Fe. δ is very sensitive to the oxidation state of Fe; for metallic Fe, ionic Fe^{3+}, and ionic Fe^{2+} typical values of δ are 0, 0.5, and 1.2 mm/s, respectively. The hyperfine field value at saturation is also dependent on the oxidation state: for Fe in a metallic environment, $H_{hf}(T=0)$ = 250−350 kOe (340 kOe for α-Fe) and for Fe^{3+} in an insulating oxide, $H_{hf}(T=0)$ = 450−550 kOe.

All the reported spectra are zero external field spectra and were recorded in the temperature range 4.2−330 K.

Synthesis

Iron(II) bis-(ethyl-2-hexyl)sulfosuccinate, $Fe(AOT)_2$, dissolved in isooctane forms reverse micelles. The addition of the same volume of aqueous phase and the micellar solution induces a phase transition. In the lower part, an anisotropic birefringent phase is observed which is supposed to be a lamellar or cylindric phases. In the upper part, an isotropic nonbirefringent reverse micellar phase is observed.

Syntheses are performed in an Ar atmosphere chamber to prevent oxidation. The crystallites are obtained by mixing, under vigorous stirring 25 mL of a 0.1 M $Fe(AOT)_2$−isooctane micellar solution to 25 mL of an aqueous solution containing $NaBH_4$ ([$NaBH_4$] = 0.4 M). Immediately after mixing, reduction of Fe^{2+} ions occurs and a black precipitate appears. It is washed with deaerated isooctane and then with acetone to remove all the surfactant. The precipitate is dried in an Ar atmosphere chamber.

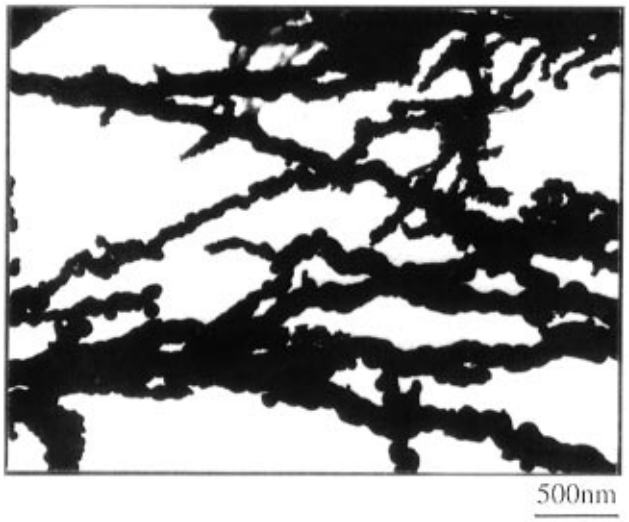

Figure 1. Transmission electron microscopy picture.

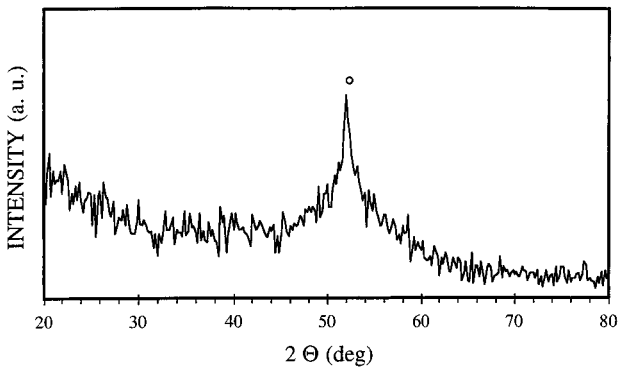

Figure 2. X-ray diffractograms with a cobalt anticathode: $\lambda_{K\alpha}$ = 0.1789 nm. (○) BCC α-Fe phase.

According to parameters controlling the iron(II) reduction by borohydride in aqueous phase, various reactions can occur although the reaction mechanism is not clearly established.[23]

Results

The TEM pattern exhibits 10−100 nm diameter particles (Figure 1). The largest are organized as elongated aggregates on a wide domain: a few microns length and approximatively 100 nm thickness. The powder X-ray diffractogram (XRD) exhibits two superposed peaks at d = 2.02 Å (Figure 2). The first one is very broad with a full width at half-maximum (fwhm) equal to approximatively 11° (2θ) asigned to an amorphous phase. The fwhm of the other one is 3.3° (2θ); it is asigned to BCC α-Fe phase. No oxide phase is detected. The same crystalline phase is detected by electron diffraction (ED).

The EELS line spectrum is recorded across a 60 nm particle (Figure 3). Figure 4 shows a perspective view of the sequence of EELS spectra acquired while the 1 nm probe is scanned across the particle. One clearly sees the oxygen K edge at 540 eV and the iron $L_{2,3}$ edge at 705 eV. Atomic concentrations of iron, boron, and oxygen are deduced from the above set of data by applying for each spectrum the conventional quantification technique consisting in measuring the specific

(21) Petit, C.; Lixon, P.; Pileni, M. P. *Langmuir* **1991**, *7*, 2620.
(22) Colliex, C.; Tencé, M.; Lefèvre, E.; Mory, C.; Gu, H.; Bouchet, D.; Jeanguillaume, C. *Microchim. Acta* **1994**, *114/115*, 71. Tencé, M.; Quartuccio, M.; Colliex C. *Ultramicroscopy* **1995**, *58*, 42.
(23) Shen, J.; Li, Z.; Yan, Q.; Chen, Y. *J. Phys. Chem.* **1993**, *97*, 8504.

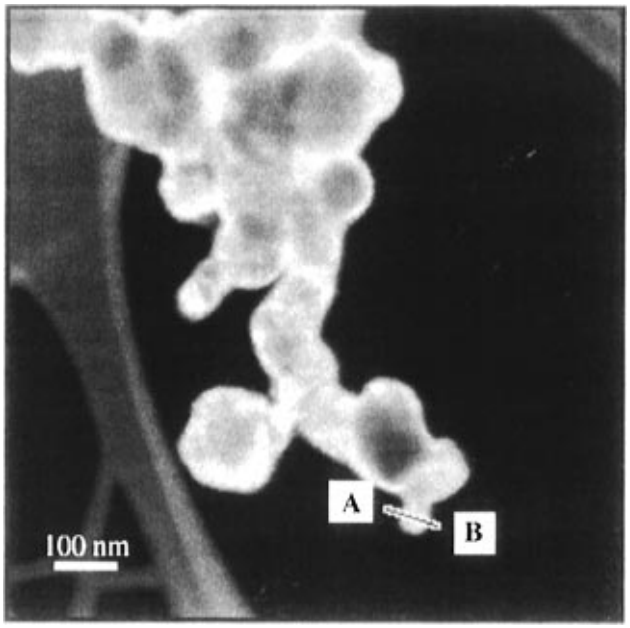

Figure 3. TEM micrograph showing a spherical particle analyzed by EELS.

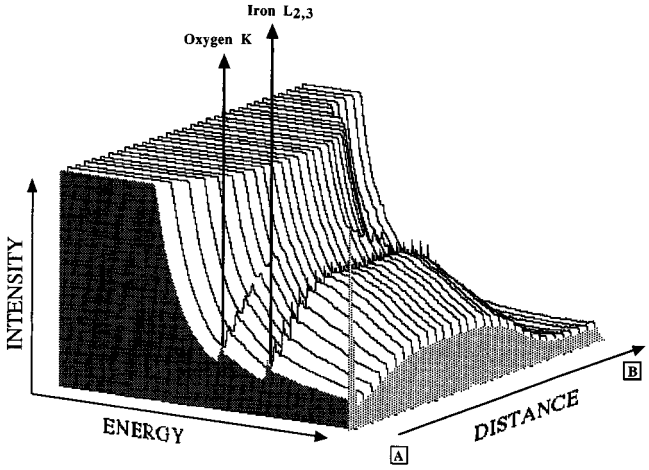

Figure 4. Perspective view of the intensities in a line-spectrum across a nanoparticle, with the iron $L_{2,3}$ and oxygen K lines at 705 and 540 eV respectively.

signal for each edge (the B−K edge line lies in the strongly decreasing slope of the background at about 185 eV) after background subtraction. Normalizing each signal with its corresponding excitation cross section leads to the determination of the relative concentrations (we assume that the total weight of these three signals amounts to 1 for each spectrum independently). From investigations by EELS performed along a line (Figure 3) it is deduced that 40 nm are made of pure iron and is surrounded by 20 nm layer of boron, oxide, and iron. We have observed a rather similar behavior for different particles chosen at random.

The results presented in Figure 5A show unambiguously that the iron atoms are in majority in the center of the particle. A phase containing iron, boron and oxygen surrounds the particle. To confirm this result, three spectra corresponding to well-defined probe positions with respect to the investigated particle are shown in Figure 5B in the first difference mode, to enhance the visibility of the weaker boron and oxygen edges. The normalization of the three spectra so that the Fe signal is equivalent shows clearly that the relative weight of

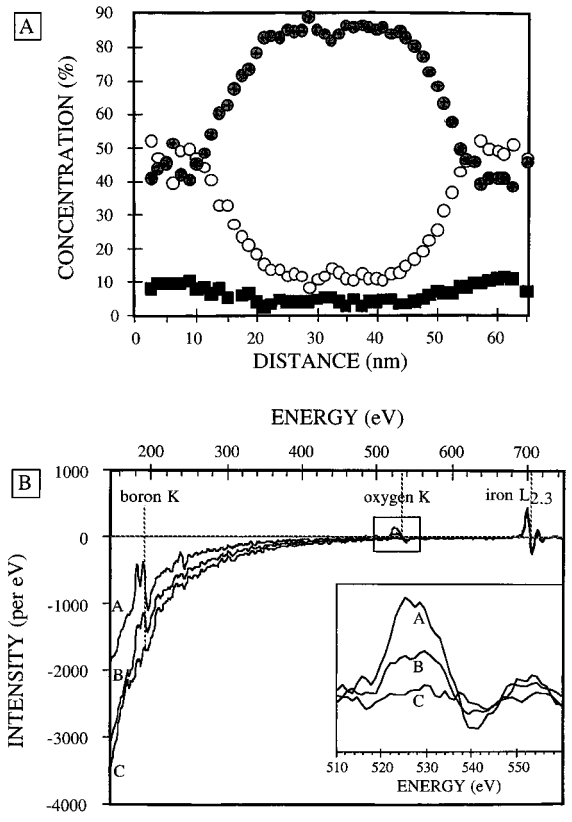

Figure 5. (A) EELS spectrum across a nanoparticle. Gray circle: Fe. Open circles: O. Black boxes: B. (B) EELS first derivative spectra normalized on $L_{2,3}$ edge showing the variation of boron and oxygen concentration from the center to the surface of the particle. (A) Surface. (B) Intermediate position. (C) Core of the particle. Insert: enhancement of oxygen K.

boron and oxygen decreases in accordance while the probe moves from the outside to the core of the particle (spectra A−C, insert in Figure 5B). This study in the first-derivative mode eliminates greatly the importance of the multiple scattering events that can bias the quantitative analysis when the specimen thickness is as high as 80−100 nm.

The ^{57}Fe Mössbauer spectra were recorded at 4.2 and 300 K. At both temperatures, the spectra can be fitted with two magnetic hyperfine sextets, of roughly equal intensities (Figure 6). One of them has narrow lines and hyperfine fields of 339 and 330 kOe at 4.2 and 300 K respectively, and a room-temperature isomer shift $\delta \approx 0$. This component is attributed to BCC α-Fe.[24] The other component shows broad lines, and a room temperature isomer shift $\delta \approx 0$. It can be fitted with a Gaussian distribution of hyperfine fields, with mean values 285 and 255 kOe at 4.2 and 300 K, respectively, characteristic of iron atoms in a metallic environment. The mean-square deviation of these distributions is 60 kOe, suggesting that this phase is amorphous.

The room-temperature magnetization measurement displays a hysteresis in Figure 7. The saturation magnetization, M_S, the remanence, M_R, and the coercive field H_C are equal to 33.5 emu/g, 5.1 emu/g, and 162 Oe, respectively.

(24) Janot, C. *L'Effet Mössbauer et ses applications*, Masson, Ed.; **1972**.

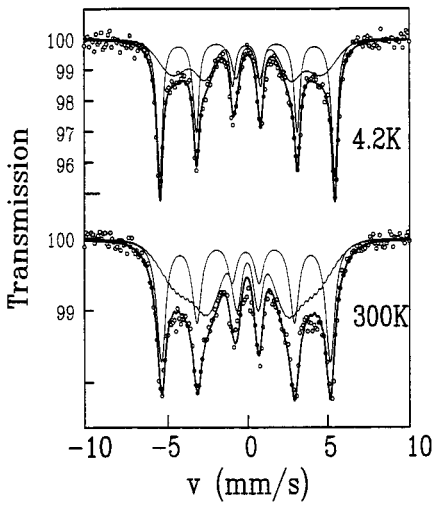

Figure 6. ^{57}Fe Mössbauer spectra at 300 and 4.2 K. The subspectrum with narrow lines corresponds to the α-Fe phase and the subspectrum with broad lines to an Fe−B amorphous alloy. The latter component has been fitted with a Gaussian distribution of hyperfine fields with mean value 285 kOe at 4.2 K and 255 kOe at 300 K. The two components have approximatively equal weights.

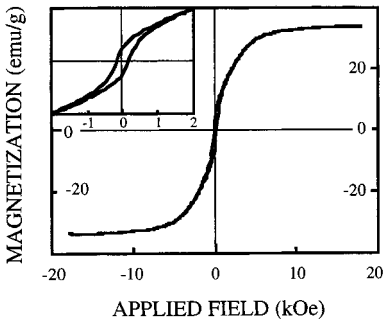

Figure 7. Room-temperature magnetization plot. The insert is a magnification of the main curve. M_S = 33.5 emu/g; M_R = 5.1 emu/g; H_C= 162 Oe.

Discussion

Syntheses performed in diphasic systems show formation of BCC α-Fe crystalline phases and $Fe_{1-x}B_x$ alloy.

The BCC α-Fe crystallites formation is demonstrated from an X-ray diffraction pattern (Figure 2) with a [110] peak. This phase also appears in Mössbauer spectra (Figure 6) as the first subspectrum.

The concentration profile deduced from EELS measurements displayed in Figure 5A can be explained following a model of a pure iron core of about 40 nm encapsulated within a shell of oxidized $Fe_{1-x}B_x$ with x on the order of 0.2. If the whole core would be made of $Fe_{1-x}B_x$, the B content profile would rather behave in accordance to the Fe one. As the boron profile varies in accordance with the oxygen one, we have actually to assume that the boron is also mostly located within this coverage layer. This is supported by the TEM pattern shown in Figure 1 in which the constrast differs from the internal core of the material compared to the interface.

By XRD, excepted BCC α-Fe no crystalline phase is detectable. A large peak of 11° (2Θ) of fwhm, centered around 52.3°, is asigned to an amorphous phase.[17] This is markedly supported by a second sextet observed by Mössbauer spectroscopy. It is assigned to a metallic Fe-based alloy. The broad Mössbauer absorption lines are characteristic of a hyperfine field distribution and reflect an amorphous phase which can be identified as a $Fe_{1-x}B_x$ alloy and characterized by low values of the hyperfine field H_{hf}.[4,15,16,20,23] The relative percentage of boron compared to iron atoms depends on the experimental conditions in which syntheses are performed.[25] The hyperfine fields[4] of the $Fe_{1-x}B_x$ alloys decrease linearly with increasing composition, x. In our experimental conditions, the hyperfine value is 255 kOe at room temperature. This corresponds to a composition of 22% of boron atoms. This is in good agreement with data obtained from EELS where the Fe/B ratio is found to be on the order of 4 within the external coverage. This corresponds to 18% of boron. These results are in good agreement to those obtained by Hadjipanayis et al.[26] from which they claim that the alloys are amorphous for a composition equal or higher to 0.20.

The saturation magnetization value shown in Figure 7 (33.5 emu/g) compared to that is relatively low obtained with bulk BCC α-Fe phase (215 emu/g).[27] This can be attributed to the presence of alloys in nanosized scale. This is supported by the following:

(i) In $Fe_{1-x}B_x$ bulk amorphous alloys the magnetic moment of iron gradually decreases down to a zero value upon increasing the boron content.[28]

(ii) For a given boron concentration, the saturation magnetization is usually lower in the amorphous state than in crystalline samples.[29]

(iii) Magnetization decreases with decreasing the particle size.[26]

(iv) A "dead layer"[30] or "spin canting"[31] due to the presence of borate,[19,20] oxide,[26,32] and surfactant at the interface favors the decrease in the magnetization saturation.

Hence by using a biphasic colloidal transition α-Fe elongated coated by $Fe_{1-x}B_x$ alloys are formed. Such a nanostructure could be useful in applications because it combines magnetic properties with an interface in which a catalytical reaction can be performed. It is impossible to conclude that this synthesis mode is the only way to control morphology and composition. However, we already demonstrated in our laboratory that the presence of a charge interface acting in a supersaturation regime is able to control the size,[33,34] morphology,[35−37] and composition[38,39] of the nanomaterial.

(25) Leslie-Pelecky, D. L.; Rieke, R. D. *Chem. Mater.* **1996**, *8*, 1770.
(26) Hadjipanayis, G. C.; Tang, Z. X.; Gangopadhay, S.; Yiping, L.; Sorensen, C. M.; Klabunde, K. J.; Kostias, A.; Papaefthymiou, V. *Studies of Magnetic Properties of Fine Particles and their relevance to Material Science*; Dormann, J. L., Fioriani, D., Ed.; **1992**, 35.
(27) Kittel, C. *Physique de l'état solide, Bordas, Paris* **1983**.
(28) Bratkovsky, A. M.; Rashkeev, S. N.; Wendin, G. *Phys. Rev. B* **1993**, *48*, 6260.
(29) Gangopadhyay, S.; Yiping, L.; Hadjipanayis, G. C.; Sorensen, C. M.; Klabunde, K. J.; Papaefthymiou, V.; Kostikas, A. *Physics and Chemistry of Finite Clusters: From Clusters to Crystals*; Kluwer Academic Publishers: Dordrecht, 1992; Vol. 1, p 743.
(30) Berkowitz, A. E.; Schuele, W. J.; Flanders, P. J. *J. Appl. Phys.* **1968**, *39*, 1261.
(31) Morrish, A. H.; Haneda, K.; Schurer, P. J. *J. Phys. Colloq.* **1976**, *37*, C6−301.
(32) Haneda, K.; *Can. J. Phys.* **1987**, *65*, 1233. Haneda, K.; Morrish, A. H. *IEEE Trans. Mag.* **1989**, *25*, 2597.
(33) Pileni, M. P. *J. Phys. Chem.* **1993**, *97*, 6961
(34) Pileni, M. P. *Langmuir*, in press

Conclusion

In this paper, it has been shown that chemical reduction of functionalized surfactant in a colloid system allowed us to obtain small metallic particles. The system chosen was $Fe(AOT)_2$/water/isooctane reduced by sodium borohydride, $NaBH_4$, in an inert atmosphere. Core−shell structured ultrafine particles (10−100 nm) were obtained. The variation of composition between the core and the surface of one particle chosen at random was investigated. BCC α-Fe is located in the center and an amorphous $Fe_{80}B_{20}$ alloy is detected at the surface. Oxidation is evidenced by presence of oxygen atoms located at the surface of the particles.

CM9701567

(35) Lisiecki, I.; Billoudet, F.; Pileni, M. P. *J. Phys. Chem.* **1996**, *100*, 4160
(36) Tanori, J.; Pileni M. P. *Adv. Mater.* **1995**, *7*, 862
(37) Tanori, J.; Pileni M. P. *Langmuir*, in press.
(38) Cizeron. J.; Pileni, M. P. *J. Phys. Chem.* **1995**, *99*, 1741
(39) Levy, L.; Hochepied, J. F.; Pileni, M. P. *J. Phys. Chem.* **1996**, 100.